Chemical Engineering Journal 158 (2010) 241–249

Contents lists available at ScienceDirect

Chemical Engineering Journal

journal homepage: www.elsevier.com/locate/cej

Dynamic modeling and process optimization of an industrial sulfuric acid plant

Anton A. Kiss[a,*], Costin S. Bildea[b], Johan Grievink[c]

[a] AkzoNobel Research, Development and Innovation, Process & Product Technology, Velperweg 76, 6824 BM, Arnhem, The Netherlands
[b] University "Politehnica" Bucharest, Centre for Technology Transfer in Process Industries, Polizu 1-7, RO-011061 Bucharest, Romania
[c] Delft University of Technology, Department of Chemical Engineering, Julianalaan 136, 2628 BL, Delft, The Netherlands

ARTICLE INFO

Article history:
Received 15 October 2009
Received in revised form 8 January 2010
Accepted 11 January 2010

Keywords:
Sulfuric acid
Adiabatic reactors
Absorption
Optimization
SOx emissions
Energy savings

ABSTRACT

The current legislation imposes tighter restrictions in order to reduce the impact of chemical process industry on the environment. In this context, this study presents the dynamic model, simulation and optimization results for an industrial sulfuric acid plant. The dynamic model, implemented in PSE *g*PROMS includes a catalytic reactor (five pass converter), heat exchangers such as economizers and feed-effluent heat exchangers, mixers, splitters and reactive absorption columns. The kinetic parameters were fitted to the real plant data, while the remaining model parameters were estimated using classical correlations. The modeling results agree very well with the real plant data.

The model implemented in *g*PROMS is useful for evaluating the dynamic behavior of the plant and for minimization of the total amount of SOx emissions. The SOx emissions could be significantly reduced by over 40% by optimizing operating parameters such as air feed flow rates or split fractions. However, only minor increases in energy production can be achieved due to the plant already operating near full capacity. The simulations also show that operational problems may occur when the process is disturbed due to production rate changes or catalyst deactivation, the non-linear response of the plant leading to sustained oscillations. Besides controllability, operability and optimization studies the *g*PROMS plant model is also useful for operator training and various scenario assessments.

1. Introduction

As the largest-volume industrial chemical produced in the world, consumption of sulfuric acid is often used to monitor a country's degree of industrialization. Sulfuric acid is produced every year in quantities larger than any other chemical [1,2]. Nowadays, the worldwide production exceeds 160 million of tonnes, with US and Asia as the top consumers (Fig. 1).

Remarkably, sulfuric acid is also a particularly corrosive and dangerous acid, with extreme environmental and health hazards if not manufactured, used, and regulated properly. Sulfuric acid has a wide range of uses including: phosphate fertilizer production, dyes, alcohols, plastics, rubber, ether, glue, film, explosives, drugs, paints, food containers, wood preservatives, soaps and detergents, pharmaceutical products, petroleum products, pulp and paper. The common lead-acid storage battery is one of the few consumer products that actually contain H_2SO_4. Sulfuric acid is also used extensively as a solvent for ores and as catalyst for petroleum refining and polymer manufacture. Note that agricultural fertilizers represent the largest single application for sulfuric acid, accounting for up to 65% of its usage. The most common process used for making phosphate fertilizers consists of two steps:

(1) Production of phosphoric acid and gypsum, by reacting phosphate rock with H_2SO_4.

$$Ca_3(PO_4)_2(s) + 3H_2SO_4(lq) + 6H_2O(lq) \rightarrow 2H_3PO_4(lq) + 3CaSO_4{\cdot}2H_2O(s) \quad (1)$$

(2) Reaction of phosphoric acid with ammonia to make ammonium phosphates.

$$2H_3PO_4 + 3NH_3 \rightarrow NH_4H_2PO_4 + (NH_4)_2HPO_4 \quad (2)$$

Sulfuric acid plants are distributed throughout the industrialized world, as follows: 35% Asia, 24% North America, 7% South and Central America, 10% Western Europe, 10% Eastern Europe, 11% Africa and 3% Oceania and Australia [1,2]. Most of the sulfuric acid plants are located near their product acid's point of use—*i.e.* near phosphate fertilizer plants, nickel ore leach plants and petroleum refineries. The reason for this is because elemental sulfur is cheaper to transport than sulfuric acid. Note also that the volatility of the sulfuric acid price is due to the small imbalances between acid demand and supply, as well as the difficulty of storing large quantities of acid. The recent large increase in price

* Corresponding author. Tel.: +31 026 366 1714; fax: +31 026 366 5871.
E-mail addresses: Tony.Kiss@akzonobel.com, tonykiss@gmail.com (A.A. Kiss).

1385-8947/$ – see front matter © 2010 Elsevier B.V. All rights reserved.
doi:10.1016/j.cej.2010.01.023

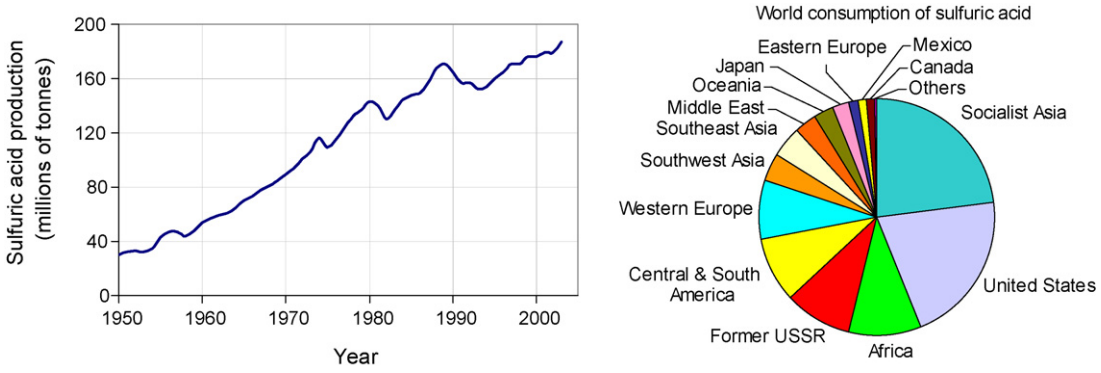

Fig. 1. Sulfuric acid production (left) and consumption (right) in the world.

is due to China's increasing demand for fertilizer, hence sulfuric acid.

The benefits of the applications of model-based optimization and control to industrial plants can be highlighted with some recent contributions. For example, model-based control was applied to temperature control in an industrial batch reactor and to product quality control in a batch crystallization [3,4]. Simon et al. [5] reported the model-based control of a liquid swelling constrained batch reactor subject to recipe uncertainties. Dynamic modeling was primarily used to make a comprehensive comparison of control strategies for Dividing-Wall Columns [6]. The dynamics and control of a new process for fatty acid esterification by dual reactive distillation are discussed by Dimian et al. [7]. Moreover, several applications of dynamic modeling to control plants of industrial significance were reported in the book of Dimian and Bildea [8].

Among other standard simulation environments used in the chemical industry, *g*PROMS has a proven track record of being successfully applied in major research areas, such as: reactive separation processes [9], pressure-swing absorption [10], polymerization processes [11], dynamic modeling [12], process design and control [13], optimization of design and operation [14], and several other application areas. For a comprehensive list of publications the reader is directed to the website of Process Systems Enterprise (www.psenterprise.com/academic/publications.html).

2. Problem statement

The literature study shows that during the last two decades the research in the area of sulfuric acid production captures interesting topics requiring reliable (dynamic) modeling, as for example: numerical-simulation of a periodic flow reversal reactor for SO_2 oxidation [15], modeling of hot and cold start-ups [16], study of unsteady-state catalytic oxidation of SO_2 by periodic flow reversal [17], modeling the oxidation of SO_2 in a trickle-bed reactor [18], modeling of SO_2 oxidation in a fixed-bed reactor with periodic flow reversal [19], modeling of SO_2 oxidation taking into account dynamic properties of the catalyst [20], oxidation of SO_2 in a trickle-bed reactor packed with activated carbon at low liquid flow rates [21], optimization studies in H_2SO_4 production [22], optimization of an adiabatic multi-bed catalytic reactor for the oxidation of SO_2 [23], simultaneous determination of SO_3 and SO_2 in flowing gases [24], model-based experimental analysis of fixed-bed reactors for SO_2 oxidation [25].

The previous studies focused either only on the SO_2 oxidation reactor or solely on the SO_3 absorption. In contrast, this study presents a complete dynamic model of an industrial sulfuric acid plant—currently operated by Phosphoric Fertilizers Industry (www.pfi.gr), as well as the results of the simulation and optimization of the plant. Due to its powerful features, *g*PROMS was selected to perform all simulation tasks [26]. The dynamic model developed in this study includes also a graphical user interface – built in Microsoft Excel – that allows scenario evaluation and operator training. The model of the complete plant was successfully used for dynamic simulations to evaluate the non-steady-state behavior of the plant and detect changes in product quality, as well as to minimize the total amount of sulfur oxides released in the atmosphere.

3. Process description

There are two major processes used for the sulfuric acid production: the lead chamber process [27] and the current contact process [28]. The main steps in the latter process consist of burning sulfur (S) in air to form sulfur dioxide (SO_2), converting SO_2 to sulfur trioxide (SO_3) using oxygen (O_2) from air, and absorbing SO_3 in water (H_2O) or a diluted solution of sulfuric acid (H_2SO_4) to form a concentrated solution of acid (>96%).

$$S(s) + O_2(g) \rightleftarrows SO_2(g) \quad \Delta H_R = -296\,810\ \text{kJ/kmol} \tag{3}$$

$$SO_2(g) + 1/2\,O_2(g) \rightleftarrows SO_3(g) \quad \Delta H_R = -96\,232\ \text{kJ/kmol} \tag{4}$$

$$SO_3(g) + H_2O(lq) \rightleftarrows H_2SO_4(lq) \quad \Delta H_R = -132\,000\ \text{kJ/kmol} \tag{5}$$

The simplified flowsheet of the industrial sulfuric acid production process consists of a sulfur burner, multi-pass converter, heat exchangers and absorbers as shown in Fig. 2.

Filtered ambient air is drawn through a high efficiency drying tower by the main compressor to remove moisture. The compressed dry air enters a refractory-lined furnace where molten sulfur is burned to produce SO_2. The hot SO_2 combustion gas is then cooled in a steam boiler to the proper temperature to promote conversion to SO_3 in the conversion step. A multi-bed catalytic adiabatic reactor is used as the SO_2 oxidation reaction is limited by the chemical equilibrium. Note that O_2 does not oxidize SO_2 to SO_3 without a catalyst, hence this is compulsory. The catalyst used here is vanadium oxide (V_2O_5) mixed with an alkali metal sulfate [29]. This mixture is supported on small silica beads, and it is a liquid at the high temperature inside the reactor [30,31]. Yet other catalysts were also reported recently [32].

The overall process is designed to give a conversion of sulfur dioxide to sulfuric acid of over 99.7%. Several conversion steps, addition of fresh air and inter-stage cooling are necessary as the reaction is reversible and exothermal [30]. SO_2 conversion is further improved and tail gas emissions are reduced through an intermediate SO_3 absorption step (Abs1). This adsorption step takes place after the fourth bed of catalyst and changes the gas composition, thus shifting the equilibrium curve to higher conversions, as shown in Fig. 3 and explained hereafter. The absorption of SO_3 is finalized

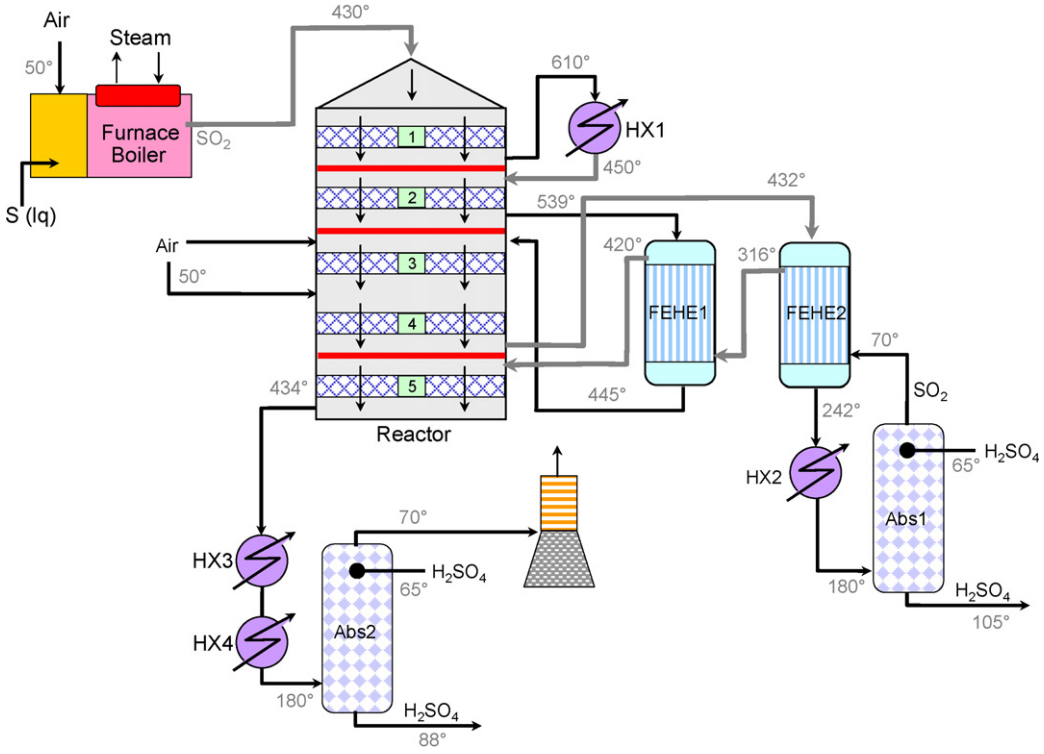

Fig. 2. Simplified flowsheet of the sulfuric acid production plant.

in the second absorber (Abs2). For heat-integration reasons, two feed-effluent heat exchangers (FEHE) are used. Remarkably, the operation of the industrial reactor follows the maximum reaction rate curve.

During operation, the flow rates of air fed to the sulfur burner and to the converter passes 3 and 4 can be changed. Moreover, it is possible to change the amount of energy that is exchanged in the feed-effluent heat exchangers FEHE1 and FEHE2 through bypassing a fraction of the cold stream (the outlet of the absorption step performed in Abs1).

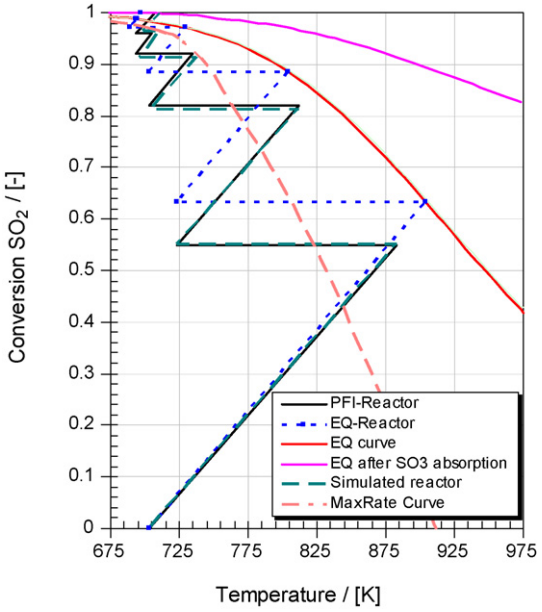

Fig. 3. Temperature-conversion diagram.

4. Dynamic model

Due to its powerful features, *g*PROMS was selected as modeling environment. *g*PROMS provides comprehensive facilities for developing, validating and executing *g*PROMS models, by performing activities such as steady-state and dynamic simulation, optimization and parameter estimation. *g*PROMS modeling language has an object-oriented character. Thus, the user defines classes of *Models* which are instantiated by *Units*. The Units can be aggregated to form complex Models [26].

According to this paradigm, the model of the sulfuric acid production plant presented in Fig. 2 is build by defining the *Models* for sulfur burner, catalytic bed, heat exchanger, feed-effluent heat exchanger and absorption column, defining the appropriate number of *Units* of each type and connecting them according to the topology of the flowsheet. To achieve the connection between the *Units*, each Model is written such that the molar flow rate, molar composition, pressure and temperature of its outlet streams are calculated within the model. Then, these variables are equated to variables associated to the downstream unit, where the values are used to compute any variable that is needed for model solving. Alternatively, *g*PROMS offers the facility to define *Stream* types, which are instantiated and used to connect units. Fig. 4 shows graphical schematics of the units used for modeling, as well as the notation used.

In the following, the main differential and algebraic equations employed in Models are given per operating unit:

(1) ***Sulfur burner*** (complete consumption of sulfur feed)

Mass balance:

$$F_{i,out} = F_{i,in} + \nu_i \cdot \xi, \quad \xi = F_{\mathrm{Sulfur},in} \tag{6}$$

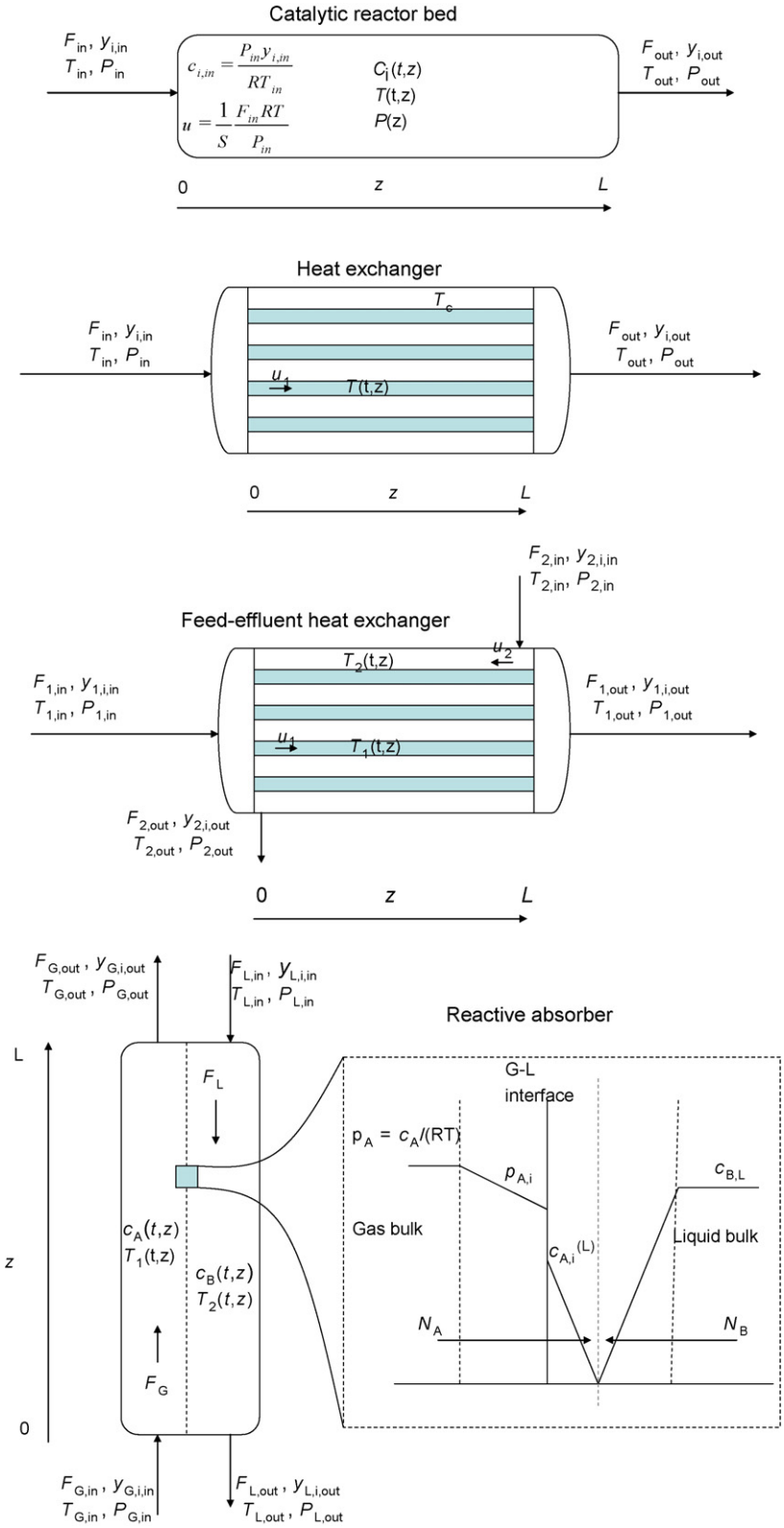

Fig. 4. Models used to describe the sulfuric acid plant.

(2) ***Catalytic reactor bed*** (pseudo-homogeneous, axial dispersion model, adiabatic operation)

Mass balance:

$$\frac{dc_i}{dt} = -u\frac{dc_i}{dz} + \rho_b \cdot \nu_i \cdot r + D_z\frac{d^2c_i}{dz^2} \tag{7}$$

Energy balance:

$$(\varepsilon \cdot \rho_f \cdot c_{p,f} + \rho_b \cdot c_{p,cat}) \cdot \frac{dT}{dt}$$

$$= -\rho_f \cdot c_{p,f} \cdot u\frac{dT}{dz} + \rho_b \cdot r \cdot (-\Delta H_r) + k_z\frac{d^2T}{dz^2} \tag{8}$$

Pressure drop:

$$\frac{dP}{dz} = -f_f \cdot \rho_f \cdot \frac{u^2}{D_p} \tag{9}$$

with the boundary conditions:

$$\text{at } z = 0: \quad -D_z\frac{dc}{dz} = u \cdot (c_{in} - c);$$

$$-k_z\frac{dT}{dz} = \rho_f \cdot c_{p,f} \cdot u \cdot (T_{in} - T) \tag{10}$$

$$\text{at } z = L: \quad \frac{dc}{dz} = 0; \quad \frac{dT}{dz} = 0; \quad \frac{dP}{dz} = 0 \tag{11}$$

A kinetic model similar to the one proposed by Froment and Bischoff [30] was used:

$$r = \frac{k_1 \cdot p_{O_2} \cdot p_{SO_2} \cdot (1 - (p_{SO_3}/K_p \cdot p_{SO_2} \cdot p_{O_2}^{1/2}))}{22.414 \cdot (1 + K_2 \cdot p_{SO_2} + K_3 \cdot p_{SO_3})^2}$$

$$[\text{kmol/(kg.cat.s)}] \tag{12}$$

The parameters of the kinetic model were adjusted such that the predicted behavior agrees with the real plant data (see Fig. 3). In this work, the following values were used:

$$K_p = \exp\left(\frac{-10.68 + 11300}{T}\right) \quad [1/\text{atm}^{1/2}] \tag{13}$$

$$k_1 = 2.1125 \times 10^5 \cdot \exp\left(\frac{-3599.78}{T}\right) \quad [\text{kmol/(kg.cat.atm}^2\text{.s)}] \tag{14}$$

$$K_2 = 14.641 \quad [\text{atm}^{-1}] \tag{15}$$

$$K_3 = 6.5775 \quad [\text{atm}^{-1}] \tag{16}$$

(3) ***Heat exchangers*** (constant temperature on the shell side, T_c)

Energy balance:

$$\rho_f \cdot c_{p,f} \cdot \frac{dT}{dt} = -\rho_f \cdot c_{p,f} \cdot u\frac{dT}{dz} - \frac{4}{D} \cdot H_w \cdot (T - T_c) \tag{17}$$

(4) ***Feed-effluent heat exchangers***

Energy balance (tube side):

$$\frac{dT_1}{dt} = -u_1\frac{dT_1}{dz} - \frac{4}{D} \cdot \frac{H_w}{\rho_1 \cdot C_{p,1}}(T_1 - T_2) \tag{18}$$

Energy balance (shell side):

$$\frac{dT_2}{dt} = u_2\frac{dT_2}{dz} + A_\nu \cdot \frac{H_w}{\rho_2 \cdot C_{p,2}}(T_1 - T_2) \tag{19}$$

(5) ***Absorbers***

The absorption model assumes one-dimensional mass and heat transport normal to the interface, thermodynamic equilibrium at the interface, and instantaneous reaction. Component A is SO_3 in gas phase, while B is H_2O in liquid phase.

Mass balance gas (A):

$$\varepsilon_G \cdot \frac{dc_A}{dt} = -\frac{4}{\pi D^2}\frac{d}{dz}(F_G \cdot C_A) - N_A \cdot A_\nu \tag{20}$$

Mass balance liquid (B):

$$\varepsilon_L \cdot \frac{dc_B}{dt} = -\frac{4}{\pi D^2}\frac{d}{dz}(F_L \cdot C_B) - N_B \cdot A_\nu \tag{21}$$

Molar flux of components:

$$N_A \cdot \left(\frac{1}{k_L} + \frac{1}{k_G \cdot H_A}\right) = \frac{p_A}{H_A} + \frac{D_B}{D_A} \cdot C_{B,L} \text{ and } N_B = N_A \tag{22}$$

Energy balance (gas):

$$\varepsilon_G \cdot \frac{dT_1}{dt} = -\frac{4}{\pi D^2} \cdot F_G\frac{dT_1}{dz} - \frac{H_w \cdot A_\nu}{\rho_G \cdot c_{p,G}}(T_1 - T_2) \tag{23}$$

Energy balance (liquid):

$$\varepsilon_L \cdot \frac{dT_2}{dt} = \frac{4}{\pi D^2} \cdot F_L\frac{dT_2}{dz} + \frac{H_w \cdot A_\nu}{\rho_L \cdot c_{p,L}}(T_1 - T_2) + \frac{N_A \cdot A_\nu}{\rho_L \cdot c_{p,L}} \cdot (-\Delta H_R) \tag{24}$$

Pressure drop:

$$\frac{dP}{dz} = -f_f \cdot \rho_f \cdot \frac{u^2}{D_p} \tag{25}$$

All the model parameters were either measured or estimated using standard correlations available in the open literature [28,33–38]. The results of the estimation fit very well in the range of general characteristics of gas–liquid reactors previously reported in literature [39]. The reference temperature and viscosity for the gas components used in the model are available in the CRC Handbook of Chemistry and Physics [40]. Moreover, UNIQUAC equation can be used in the whole concentration range for the calculation of vapor–liquid equilibrium in aqueous sulfuric acid solutions [41].

The plant model was solved in *g*PROMS. The steady-state solution is found by equating to zero the time derivatives of the model Eqs (6)–(25). The spatial coordinate is automatically discretized by the solver (first order, backwards finite differences method was used) and the resulting system of algebraic equations is solved by a non-linear solver using block decomposition (BDNLSOL). Convergence is achieved even for very rough initial approximation of the model unknowns, for example flat temperature and concentration profiles along the reactor. Finding the steady-state solution takes only a few seconds. *g*PROMS offers facilities to save the solution of one simulation in order to be used as the initial guess for the next run. This further reduces the solution time.

The solution of the dynamic model is found by discretizing the spatial coordinate and integrating the resulting set of differential and algebraic equations. SRADAU, a fully implicit variable-step Runge-Kutta method was used. The method is efficient for solution of differential equations arising from discretization of PDE with strongly advective terms and handles well discontinuities. About 1 min. of computing time is necessary to simulate 1 h of operation. The model is robust, convergence being easily achieved when step changes of reasonable magnitude were imposed on the control variables. The sequential quadratic programming method included in CVP_MS (Control Vector Parameterisation—Multiple-Shooting) dynamic optimization solver was used for the optimization problems described in the next section, a solution being obtained in about 1 h of computer time.

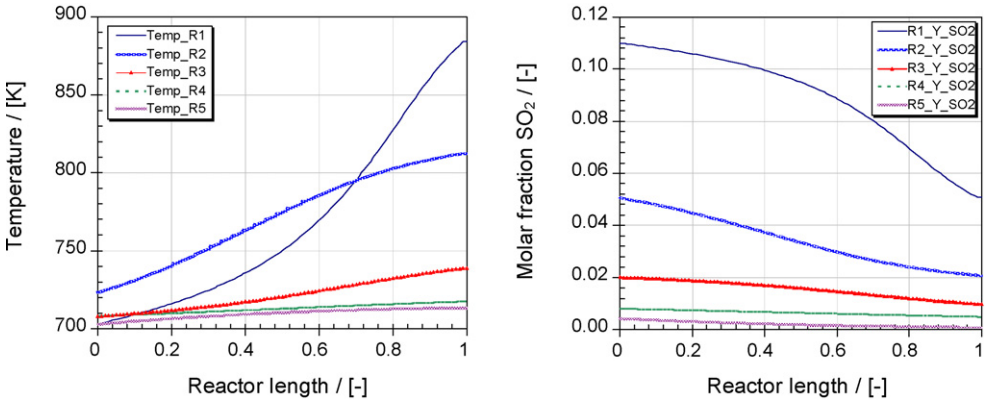

Fig. 5. Temperature and composition profiles along the oxidation reactor.

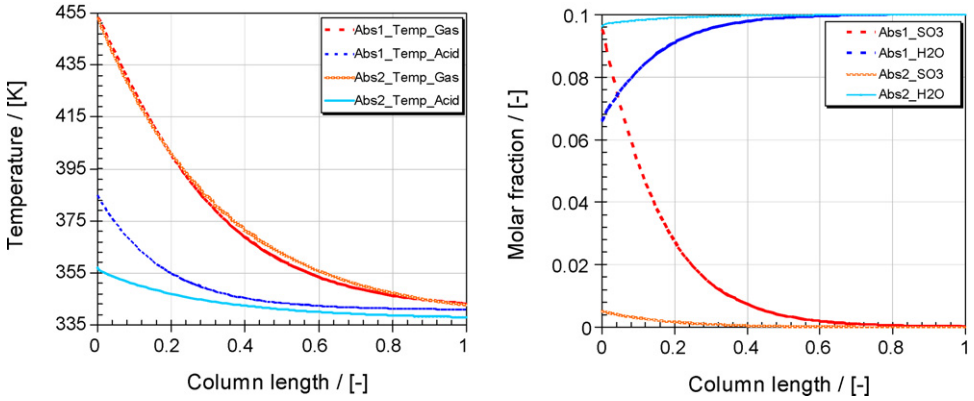

Fig. 6. Temperature and composition profiles along the two absorption columns.

5. Results and discussion

The path of the reaction can be conveniently shown in the X–T diagram, as illustrated by Fig. 3. One equilibrium curve corresponds to each composition of the reaction mixture at reactor inlet. The operating lines represent the simultaneous increase of conversion and rise of temperature which take place along each catalytic bed. The slope of the operating lines is proportional to the reciprocal value of the adiabatic temperature rise, $1/\Delta T_{ad}$. The horizontal lines represent cooling of the reaction mixture which takes place in the external heat exchangers or by injection of fresh cold air. The evolution of temperature and conversion in the industrial reactor is represented in Fig. 3 by a continuous line. The dashed line represents the same variables as predicted by the model. The model practically coincides with the industrial reactor for the first two catalytic beds, while the error is very small for the next three beds. For a given inlet composition, the operating lines can approach the equilibrium curve (dotted line in Fig. 3) but can never cross it. The intermediate SO_3 absorption shifts upwards the equilibrium curve and therefore allows higher conversions. Fig. 5 presents the steady-state temperature and composition profiles along the SO_2 oxidation reactor. The highest temperatures are reached at the end of the first and second catalytic bed, the following steps having less impact on conversion and temperature. Along with the increased conversion, the SO_2 concentration is reduced from about 11% at the reactor inlet down to less than 0.02%.

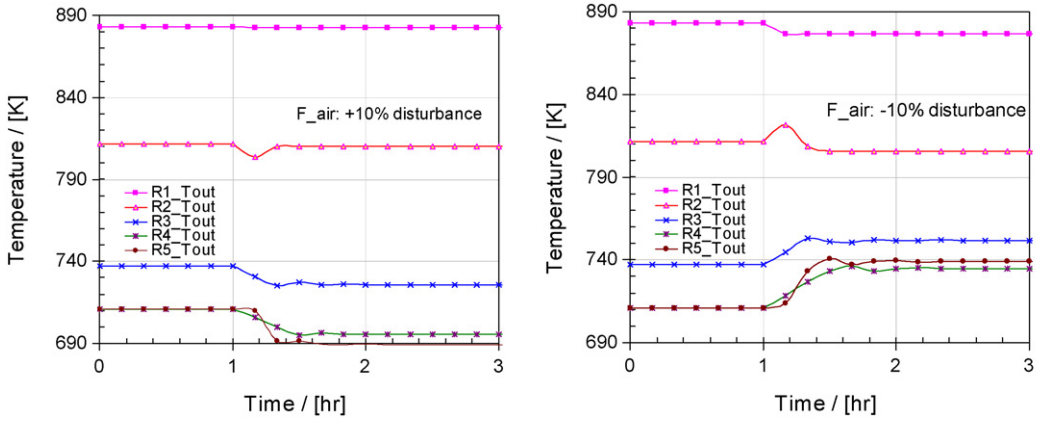

Fig. 7. Reactor temperatures profile, for ±10% changes in air feed flow rate (final case).

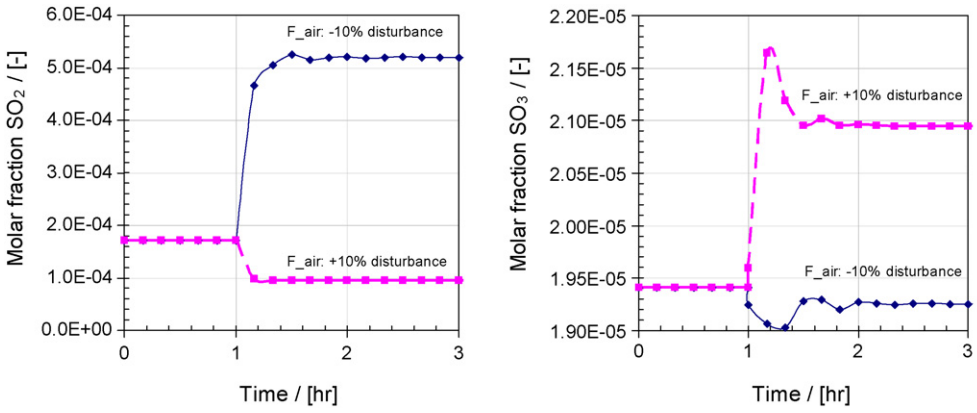

Fig. 8. SOx composition after absorption, for ±10% disturbance in the air feed flow rate.

Similarly, the steady-state temperature and composition profiles along the two absorption columns are shown in Fig. 6. Counter-current operation is used in both absorbers. The SO_3 concentration is reduced from 9.81% to 0.01% in the intermediate absorber, and from 0.44% to ppm levels in the final absorber. Note that the dimensionless length is in fact the ratio between any given length and the total absorber length.

The dynamic simulation shows that the nominal operating point of the plant is stable. When the plant is disturbed, a new steady-state is reached in less than 1 h. Fig. 7 presents simulation results for the temperature at the exits of the catalytic beds, when the flow rate of air fed to the sulfur burner is increased or decreased by 10%.

The molar fractions of SO_2 and SO_3 at the outlet of the final absorption column are presented, for similar disturbances, in Fig. 8. Note the non-symmetrical response ($-50\% \cdots +200\%$ for SO_2) to these ±10% disturbances. However, the composition reaches a new steady-state in a relatively short settling time of less than 1 h.

Multi-variable optimization was performed for several production rates, corresponding to the amount of sulfur fed into the plant (nominal value and ±5-10% changes). Five key variables were identified and manipulated accordingly to carry out the optimization:

- the amount of air fed into the sulfur burner,
- the flow rates of air fed into converter pass 3 and 4,
- the split fractions (by-pass) for cold streams entering the gas-gas heat exchangers (FEHE1 and FEHE2).

It should be remarked that the plant produces a significant amount of energy in the sulfur burner and the heat exchangers HX1–HX4. Therefore, the first optimization run aimed at maximizing the amount of energy produced. Increasing energy production is equivalent to maximizing the amount of SO_2 converted into products. A flat optimum is expected because practically the entire amount of heat generated in the reaction is recovered due to tight energy integration. As the conversion of the process is already very high, almost 99.85%, any further increase is insignificant. Therefore, not surprisingly, the energy production can be increased only by almost one percent.

The second optimization target sought to minimize the total amount of SOx released in atmosphere (*i.e.* not absorbed in the final absorption column). The optimization results reveal that – for the nominal operating point – the flow rate of air fed to sulfur burner should be increased by 30%. Moreover, the flow rates of air entering the catalytic beds 3 and 4 must increase by 80% and decrease by 10%, respectively. Finally, the cold streams should not be split to by-pass the heat exchangers. The conversion profiles in the reactor for changes of ±10% in the feed flow rate are given in Fig. 9 (left). Remarkably, the SOx emissions can be drastically reduced by ∼40% – in the nominal case – or even more, depending on the operating region (Fig. 9). Therefore, the industrial sulfuric acid plant can be now fully exploited even at larger production rates, while respecting the current ecological restrictions.

6. Discussion of the dynamic behavior

It should be noted that the tight heat-integration can lead to operational difficulties when the plant is not well designed. For example, we considered the kinetics presented in Froment and

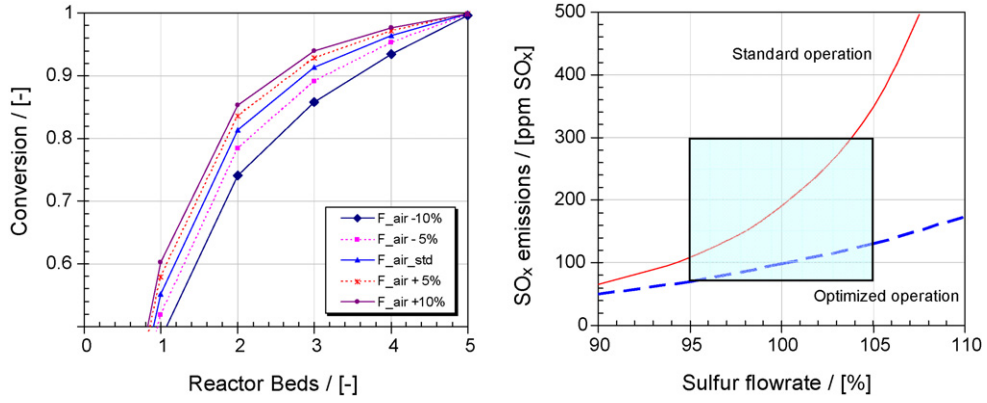

Fig. 9. Conversion profiles in the reactor, for ±10% changes in the air feed flow rate (left). SOx emissions (lower is better) before and after optimization at various feed flow rates (right).

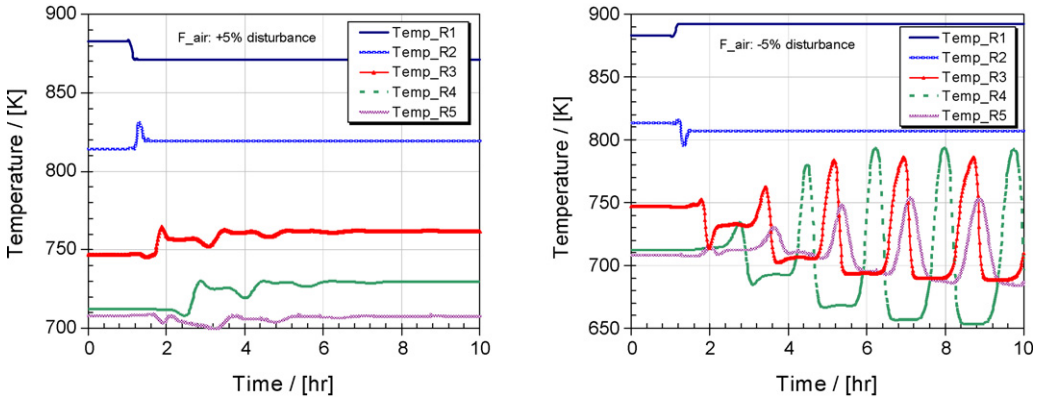

Fig. 10. Evolution of bed-outlet temperature ±5% change in air feed flow rate (kinetics taken from [30]).

Bischoff and designed a plant which achieves the same performance as the plant discussed in the previous sections. Although the nominal operating point is stable, the response of the plant is non-linear and, for certain disturbances, sustained oscillations are observed. Fig. 10 presents the temperature at the exit of the catalytic bed, for ±5% changes of the air feed flow rate. Obviously, these oscillations are not acceptable since they propagate from the reactor to absorbers, rendering the plant unstable and the product off-spec. Other disturbances that may have a similar effect are production rate changes, catalyst deactivation, or variation of air feed flow rates caused by day–night or summer–winter temperature differences and constant volumetric flow operation.

Morud and Skogestad [42] reported a similar behavior of a multi-bed, heat-integrated industrial ammonia reactor, where small changes of operating conditions led to onset of sustained oscillations. The non-linear behavior was explained by the presence of an inverse response for the temperature through the reactor beds, combined with the positive energy feedback induced by the two feed-effluent heat exchangers. Nevertheless, a complete non-linear analysis would be required to reveal all steady-states that are possible [43–48].

7. Conclusions

This work presents the complete model of an industrial sulfuric acid plant, as well as the simulation and optimization results. Process Systems Enterprise *g*PROMS was successfully used – as an advanced process modeling, simulation and optimization environment – for dynamic simulations to evaluate the non-steady-state behavior of the plant and detect changes in product quality, as well as for optimization of the total amount of SOx released in the atmosphere. In addition, a Microsoft Excel interface was developed to allow a more user-friendly interaction, thus making the model suitable for operator training.

The dynamic model includes a catalytic reactor (five pass converter), heat exchangers such as economizers and feed-effluent heat exchangers, mixers, splitters and reactive absorption columns. As no suitable kinetics information was available, the kinetic parameters were fitted to the real plant data, while the remaining parameters required for modeling were estimated using classical correlations. The results show that an excellent agreement exists between the real plant data and the results of the simulations, the relative error being typically below 1%.

Along with minor benefits in energy production, the amount of SOx emissions could be significantly reduced by ~40% just by optimizing operating parameters such as air feed flow rates or split fractions. Besides controllability, operability and optimization studies the plant model coded in *g*PROMS is also useful for operator training and scenario assessments.

The robust dynamic model developed in this work may be further used for:

- Controllability analysis to determine the controllability of the plant and the possible improvements of the control structure, as well as optimal control policy.
- Other dynamic simulations, to detect potential sensitivity problems and which model parameters have greater importance.
- Operator training, due to the Excel interface that plays the role of a control panel that simulates the real plant behavior for any change of model parameters.
- Other optimization studies, such as tuning the amount of energy produced by the plant or optimize the air feed policy accounting for day/night temperature variations.

Notation

a_p	specific surface area of the packing (m^2/m^3)
A_v	specific area (m^2/m^3)
c_i	concentration of component i (kmol/m^3)
c_p	specific heat capacity (J/kg·K)
D	diameter (m)
D_i	diffusion coefficient (component i)
D_z	axial dispersion coefficient (m^2/s)
f_f	friction factor
H_A	Henry constant for component A
H_w	total heat transfer coefficient (W/m^2·K)
$k_{G/L}$	partial mass transfer coefficient (gas or liquid phase)
L	length of the operating unit
N_i	molar flux of component i
P	pressure (Pa)
p_i	partial pressure component i (Pa)
r	reaction rate (kmol/kg.cat)
R	Rydberg constant (8.3145 J/mol·K)
Re	Reynolds number
t	time (s)
T	temperature (K)
T_c	temperature coolant (K)
u	velocity (m/s)
α	individual heat transfer coefficient (W/m^2·K)
λ	thermal conductivity (W/m·K)
ΔH_r	enthalpy of reaction (J/mol)
ε	void fraction
ρ_b	density of the bulk (bed) catalyst (kg/m^3)
ρ_f	density of the fluid (kg/m^3)
ν_i	stoichiometric coefficient
λ	thermal conductivity (W/m·K)
μ	dynamic viscosity (Pa·s)

Acknowledgement

This project was funded by the European Commission (OPT-ABSO Project, Contract no. G1RD-CT-2001-00649). We also thank Phosphoric Fertilizers Industry and Process Systems Enterprise Ltd. for the technical assistance.

References

[1] W.G. Davenport, M.J. King, Sulfuric Acid Manufacture, Elsevier, 2005.
[2] S.R.I. Consulting, CEH Marketing Research Report Sulphuric Acid, Chemical Economics Handbook, SRI Consulting, Menlo Park, CA, USA, 2006.
[3] Z.K. Nagy, B. Mahn, R. Franke, F. Allgower, Efficient output feedback nonlinear model predictive control for temperature control of industrial batch reactors, Control Engineering Practice 15 (2007) 839–859.
[4] Z.K. Nagy, Model based robust control approach for batch crystallization product design, Computers & Chemical Engineering 33 (2009) 1685–1691.
[5] L.L. Simon, Z.K. Nagy, K. Hungerbuhler, Model based control of a liquid swelling constrained batch reactor subject to recipe uncertainties, Chemical Engineering Journal 153 (2009) 151–158.
[6] R.C. van Diggelen, A.A. Kiss, A.W. Heemink, Comparison of control strategies for dividing-wall columns, Industrial & Engineering Chemistry Research 49 (2010) 288–307.
[7] A.C. Dimian, C.S. Bildea, F. Omota, A.A. Kiss, Innovative process for fatty acid esters by dual reactive distillation, Computers & Chemical Engineering 33 (2009) 743–750.
[8] A.C. Dimian, C.S. Bildea, Chemical Process Design—Computer-Aided Case Studies, Wiley-VCH, Weinheim, 2008.
[9] C.P. Almeida-Rivera, J. Grievink, Process design approach for reactive distillation using economics, exergy and responsiveness optimization, Industrial & Engineering Chemistry Research 47 (2008) 51–65.
[10] Q. Huang, A. Malekian, M. Eic, Optimization of PSA process for producing enriched hydrogen from plasma reactor gas, Separation and Purification Technology 62 (2008) 22–31.
[11] M. Asteasuain, A. Brandolin, Modeling and optimization of a high-pressure ethylene polymerization reactor using gPROMS, Computers & Chemical Engineering 32 (2008) 396–408.
[12] R.D. Moita, H.A. Matos, C. Fernandes, C.P. Nunes, N.J. Pinho, Dynamic modelling and simulation of a heated brine spray system, Computers & Chemical Engineering 33 (2009) 1323–1335.
[13] A. Lawal, M. Wang, P. Stephenson, H. Yeung, Dynamic modelling of CO_2 absorption for post combustion capture in coal-fired power plants, Fuel 88 (2009) 2455–2462.
[14] M.S. Tanvir, I.M. Mujtaba, Optimisation of design and operation of MSF desalination process using MINLP technique in gPROMS, Desalination 222 (2008) 419–430.
[15] J.D. Snyder, B. Subramaniam, Numerical-simulation of a periodic-flow reversal reactor for sulfur-dioxide oxidation, Chemical Engineering Science 48 (1993) 4051–4064.
[16] K. Gosiewski, Dynamic modeling of industrial SO_2 oxidation reactors. 1. Model of hot and cold start-ups of the plant, Chemical Engineering & Processing 32 (1993) 111–129.
[17] H.X. Wu, S.Z. Zhang, C.Y. Li, Study of unsteady-state catalytic oxidation of sulfur dioxide by periodic flow reversal, Canadian Journal of Chemical Engineering 74 (1996) 766–771.
[18] P.V. Ravindra, D.P. Rao, M.S. Rao, A model for the oxidation of sulfur dioxide in a trickle-bed reactor, Industrial & Engineering Chemistry Research 36 (1997) 5125–5132.
[19] R.Y. Hong, X. Li, H.Z. Li, W.K. Yuan, Modeling and simulation of SO_2 oxidation in a fixed-bed reactor with periodic flow reversal, Catalysis Today 38 (1997) 47–58.
[20] N.V. Vernikovskaya, A.N. Zagoruiko, A.S. Noskov, SO_2 oxidation method. Mathematical modeling taking into account dynamic properties of the catalyst, Chemical Engineering Science 54 (1999) 4475–4482.
[21] Y. Suyadal, H. Oguz, Oxidation of SO_2 in a trickle bed reactor packed with activated carbon at low liquid flow rates, Chemical Engineering & Technology 23 (2000) 619–622.
[22] A.A. Kiss, C.S. Bildea, P.J.T. Verheijen, Optimization studies in sulphuric acid production, Computer Aided Chemical Engineering 21A (2006) 736–742.
[23] A. Nodehi, M.A. Mousavian, Simulation and optimization of an adiabatic multi-bed catalytic reactor for the oxidation of SO_2, Chemical Engineering & Technology 30 (2007) 84–90.
[24] J.G. Ibanez, C.F. Batten, W.E. Wentworth, Simultaneous determination of SO_3 and SO_2 in a flowing gas, Industrial & Engineering Chemistry Research 47 (2008) 2449–2454.
[25] J.C. Schoneberger, H. Arellano-Garcia, G. Wozny, S. Korkel, H. Thielert, Model-based experimental analysis of a fixed-bed reactor for catalytic SO_2 oxidation, Industrial & Engineering Chemistry Research 48 (2009) 5165–5176.
[26] Ltd. Process Systems Enterprise, gPROMS Advanced User Guide, 2009.
[27] E.M. Jones, Chamber process manufacture of sulfuric acid, Industrial & Engineering Chemistry 42 (1950) 2208–2210.
[28] Kirk Othmer, Encyclopedia of Chemical Technology, vol. 22, 3rd edition, John Wiley & Sons, 1984.
[29] G.A. Bunimovich, N.V. Vernikovskaya, V.O. Strots, B.S. Balzhinimaev, Y.S. Matros, SO_2 oxidation in a reverse-flow reactor—influence of a vanadium catalyst dynamic properties, Chemical Engineering Science 50 (1995) 565–580.
[30] G.F. Froment, K.B. Bischoff, Chemical Reactor Analysis and Design, John Wiley & Sons, 1979 (Chapter 11).
[31] A. Christodoulakis, S. Boghosian, Molecular structure of supported molten salt catalysts for SO_2 oxidation, Journal of Catalysis 215 (2003) 139–150.
[32] T.L. Jorgensen, H. Livbjerg, P. Glarborg, Homogeneous and heterogeneously catalyzed oxidation of SO_2, Chemical Engineering Science 62 (2007) 4496–4499.
[33] C.R. Wilke, P. Chang, Correlation of diffusion coefficients in dilute solutions, AIChE Journal 1 (1955) 264–270.
[34] K. Onda, H. Takeuchi, Y. Okumoto, Mass transfer coefficients between gas and liquid phases in packed columns, Journal of Chemical Engineering Japan 1 (1968) 56–62.
[35] R. Taylor, R. Krishna, Multicomponent Mass Transfer, John Willey & Sons, 1993.
[36] J.K. Klassen, Z. Hu, L.R.J. Williams, Diffusion coefficients for HCl and HBr in 30 wt% to 72 wt% sulfuric acid at temperatures between 220 and 300 K, Journal of Geophysical Research 103 (1998) 16197–16202.
[37] R.H. Perry, D.W. Green, J.O. Maloney, Perry's Chemical Engineers' Handbook, 7th edition, McGraw-Hill, 1999.
[38] F.P. Incropera, D.P. DeWitt, Fundamentals of Heat and Mass Transfer, 4th edition, John Wiley & Sons, 2000 (Chapter 11).
[39] G. Bozga, O. Muntean, Chemical Reactors, vol. 2, Editura Tehnica, Bucharest, 2001.
[40] Chemical Rubber Company (CRC), in: Weast, C. Robert (Eds.), CRC Handbook of Chemistry and Physics, 65th edition, CRC Press, Inc., Boca Raton, Florida, 1984.
[41] F.L.P. Pessoa, C.E.P.S. Campos, A.M.C. Uller, Calculation of vapor–liquid equilibria in aqueous sulfuric acid solutions using the UNIQUAC equation in the whole concentration range, Chemical Engineering Science 61 (2006) 5170–5175.
[42] J.C. Morud, S. Skogestad, Analysis of instability in industrial ammonia reactors, AIChE Journal 44 (1998) 888–895.
[43] C.S. Bildea, A.C. Dimian, Stability and multiplicity approach to the design of heat-integrated PFR, AIChE Journal 44 (1998) 2703–2712.
[44] C.S. Bildea, A.C. Dimian, P.D. Iedema, Nonlinear behavior of reactor-separator-recycle systems, Computers & Chemical Engineering 24 (2000) 209–215.
[45] A.A. Kiss, C.S. Bildea, A.C. Dimian, P.D. Iedema, State multiplicity in CSTR-separator-recycle polymerization systems, Chemical Engineering Science 57 (2002) 535–546.
[46] A.A. Kiss, C.S. Bildea, A.C. Dimian, P.D. Iedema, State multiplicity in PFR-separator-recycle polymerization systems, Chemical Engineering Science 58 (2003) 2973–2984.
[47] A.A. Kiss, C.S. Bildea, A.C. Dimian, P.D. Iedema, Design of recycle systems with parallel and consecutive reactions by non-linear analysis, Industrial & Engineering Chemistry Research 44 (2005) 576–587.
[48] A.A. Kiss, C.S. Bildea, A.C. Dimian, Design and control of recycle systems by non-linear analysis, Computers & Chemical Engineering 31 (2007) 601–611.